Journal of the Brazilian Society of Mechanical Sciences and Engineering (2025) 47:131
https://doi.org/10.1007/s40430-025-05432-0

TECHNICAL PAPER

Optimization of thrust and fuel efficiency in low-altitude UAV engines through experimental design and statistical analysis

Burak Öztürk[1] · **Fatih Öncü**[1]

Received: 9 November 2024 / Accepted: 28 January 2025 / Published online: 18 February 2025

Abstract

With advancements in UAV technology, their applications in both defense and civilian sectors have expanded rapidly. These vehicles are powered by engines with diverse cylinder configurations, fuel capacities, and material characteristics. For low-altitude, small-scale UAVs, two-stroke engines are commonly preferred due to their high payload capacity and extended flight durations of 3–6 h, generally outperforming electric motors. The performance of gasoline-powered UAVs is influenced by critical factors such as engine temperature, thrust generation, and fuel consumption. This study focuses on a typical engine used in medium-sized, low-altitude UAVs, widely adopted across the globe. Researchers developed a prototype engine by increasing the fuel intake volume and enhancing cooling mechanisms to improve overall performance. The performance of both the original and modified engines was thoroughly evaluated under varying operational conditions, including different propeller types, sizes (23–8 inch and 24–10 inch), and rotations per minute (3000–5000 RPM). Key metrics such as thrust, fuel consumption, engine temperature, and RPM were systematically measured using a specially designed test setup equipped with advanced sensors and real-time data acquisition systems. To maximize flight endurance with minimal fuel consumption, response surface methodology and analysis of variance (ANOVA) were employed. The study identified an optimal operating speed of 4000 RPM, which resulted in a 47% performance improvement. At this speed, fuel consumption for a standard 4-h low-altitude flight was reduced from 2.51 to 1.86 L, demonstrating significant efficiency gains. ANOVA results revealed that propeller type significantly impacts engine performance, with propeller variations accounting for 86% of engine temperature changes. Additionally, optimized propeller designs achieved a 7% reduction in fuel consumption. This research underscores the potential of targeted engine and propeller modifications to significantly enhance UAV efficiency, providing valuable insights for future UAV development and operational strategies.

Keywords UAV · Engine · Fuel consumption · RSM

1 Introduction

Today, unmanned aerial vehicles (UAVs) are autonomous systems designed to operate without onboard pilots, either managed remotely or navigating predefined routes independently. Recent advancements have enabled many UAVs to incorporate artificial intelligence (AI), enhancing their autonomous capabilities [1, 2]. Also referred to as drones or robotic aircraft, UAVs have been widely adopted in civilian and military sectors, thanks to significant developments in radio and communication technologies that have facilitated global deployment [3, 4].

The evolution of modern UAVs gained momentum during the Cold War. The US-produced QH-50, initially developed as a training target during the Korean War, was later repurposed for reconnaissance in the Vietnam War. In 1973, Israel entered the UAV technology field by utilizing American UAVs to identify enemy positions and anti-aircraft defenses, a pivotal advancement that spurred further development. In subsequent conflicts, such as those in Afghanistan and Iraq, UAVs were deployed for counter-terrorism and precision targeting operations [5, 6]. Initially developed for military applications, UAVs have rapidly expanded into civilian sectors, a pattern common to many technological innovations. They are now essential in

Technical Editor: Sunetra Sarkar.

✉ Burak Öztürk
burak.ozturk@bilecik.edu.tr

[1] Metallurgical and Materials Engineering, Bilecik University, Bilecik, Turkey

diverse areas, including agriculture, entertainment, intelligence, and logistics. Furthermore, UAVs play a critical role in disaster response and environmental management, supporting emergency operations and natural disaster mitigation efforts [7–9].

Unmanned aerial vehicles (UAVs) generally achieve the necessary thrust for flight through electric, piston, or jet engines. UAVs powered by oil engines typically have a wingspan exceeding 5 m; smaller designs are impractical due to high fuel consumption. Conversely, electric motor-powered UAVs face limitations from additional battery weight and reduced flight duration, making them more suitable for short-range, lightweight transport tasks. UAVs with wingspans between 3 and 5 m often use piston engines, which provide longer flight durations and greater payload capacity, enabling operation times of approximately 3–6 h [10–12].

For low-altitude surveillance missions, UAVs equipped with 61 cc (or 50–70 cc) piston engines are particularly effective. These configurations allow for sustained operations of up to 4 h over distances of up to 180 km. This setup has proven valuable not only for surveillance but also for specialized kamikaze missions, where UAVs may carry explosive payloads of up to 10 kg (Fig. 1). As a result, piston-engine UAVs strike an optimal balance between endurance and payload capacity, making them indispensable for both surveillance and tactical applications in low-altitude, medium-range contexts.

This study aims to investigate the performance and fuel efficiency of piston-engine UAVs in low-altitude applications. It focuses on factors such as engine cooling, fuel intake optimization, and propeller configurations. By identifying optimal parameters to extend airborne time while minimizing fuel consumption, this research contributes to enhancing UAV effectiveness in both civilian and military contexts.

Optimal engine design plays a pivotal role in achieving the ideal compression ratio, which directly enhances thrust force, allowing UAVs to carry heavier payloads and achieve higher speeds. Current research into UAV engines is shaping future advancements in the field. For instance, researchers have studied the tribological properties of pistons and cylinders, key components influencing engine efficiency, by testing various aluminum alloys [13]. Significant improvements were made by incorporating graphite carbon fiber into AA2000 series aluminum and adding iron (Fe) and manganese (Mn) to LM13 alloys, enhancing wear resistance and minimizing performance losses. Silva's research further examined fatigue-related damage in gasoline and diesel engine pistons, identifying mechanical fatigue, temperature fluctuations, and design flaws as primary causes [14]. Additionally, studies investigating aluminum-forged pistons revealed that rapid temperature and pressure changes in the combustion chamber lead to deformations such as hardness loss, softening, and erosion, with the severity dependent on surface roughness [15]. These findings underscore the critical importance of material selection and design in improving UAV engine durability and efficiency, paving the way for more resilient systems.

Research on durable and long-lasting piston engines for UAVs has also focused on structural and thermal analysis of essential components. Optimizing these components has enabled researchers to meet emission standards, maximize efficiency, and reduce environmental impact [16]. Hermawan et al. investigated the stresses caused by pressure and thermal loads on pistons, connecting rods, and crankshafts in four-stroke diesel engines [17]. Similarly, Nageswararao and Mukesh used ANSYS Workbench 15.0 to model temperature

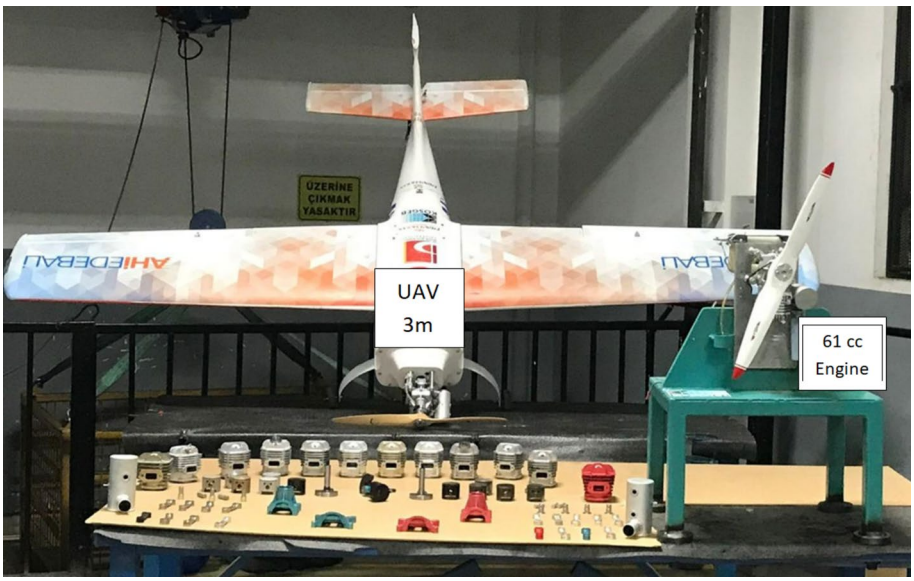

Fig. 1 A UAV with a single-cylinder 61-cc engine

distribution in internal combustion engine cylinders, highlighting the impact of heat transfer within the combustion chamber [18]. Further studies explored crankshaft journal failures in ULM aircraft engines, attributing breakage to material fatigue at high speeds [19]. Esfahanian and colleagues calculated heat transfer to engine pistons using three different combustion boundary conditions to analyze thermal behavior [20].

The literature includes numerous studies on UAV flight planning, durations, and efficiency. The increasing complexity and operational demands of unmanned aerial vehicles (UAVs) have driven extensive research into optimization techniques, aerodynamic performance improvements, and cost-effective mission planning strategies. Various methodologies, including bio-inspired algorithms, innovative wing designs, and advanced control systems, have been explored to enhance UAV capabilities. The percentile-based immune plasma algorithm (pIPA) was introduced as a novel optimization method, effectively solving engineering challenges such as UAV path planning by outperforming conventional techniques in determining optimal parameters [21]. Following this, the Extended Immune Plasma Algorithm (ExtIPA) was developed for unmanned combat aerial vehicles (UCAVs). This approach addressed challenges like enemy threats, flight kinematics, and fuel constraints, significantly improving path planning efficiency and accuracy [22]. Aerodynamic advancements have also been a key focus area. Morphing wing designs, combined with machine learning techniques such as k-Nearest Neighbor (k-NN), have shown substantial improvements in aerodynamic performance and trajectory tracking for fixed-wing UAVs [23]. Similarly, plasma actuators were studied for optimizing airfoil performance, achieving remarkable increases in lift-to-drag ratios and lift coefficients through active flow control techniques [24]. In mission planning, the European Space Agency (ESA) demonstrated how reusable software kernels could reduce costs and improve adaptability for various mission types [25]. Additionally, revolutionary approaches to mission operations have been proposed, advocating for early integration of operational concepts into spacecraft design to eliminate labor-intensive processes and lower expenses [26].

Control system advancements for UAVs include PID control algorithms developed for quadcopters. These algorithms enhanced trajectory tracking and stability, particularly in challenging environments, proving their effectiveness in autonomous UAV operations. Together, these studies provide valuable insights into UAV performance optimization, aerodynamic efficiency, and cost reduction, contributing to advancements in both military and civilian UAV applications. The study evaluated the energy and exergy performance of turbo-diesel engines used in UAVs. The energy efficiency was found to be 43.16%, while the exergy efficiency was 40.65%. Fuel losses and sustainability factors were analyzed, highlighting the superior performance of turbo-diesel engines over piston-prop engines [27]. An analytical method was developed for the sizing of a UAV and its turboprop engine. The study examined engine efficiency, specific fuel consumption, and flight parameters. Results indicated high accuracy in weight, size, and endurance predictions, with specific focus on compressor pressure ratio and turbine inlet temperature [28].

Unmanned aerial vehicles (UAVs) have become indispensable tools in both defense and civilian sectors, achieving significant technological advancements in recent years. However, efforts to enhance UAV performance, particularly in engine technologies, face several challenges. Key requirements such as high energy efficiency, optimized fuel consumption, extended flight endurance, and thermal stability have become essential in the design and development of UAV engines. Despite these demands, current engines often suffer from inefficiencies in fuel consumption, inadequate cooling mechanisms, and limited adaptability, which constrain the operational effectiveness of UAVs and underscore the need for energy-efficient, performance-oriented solutions.

This study aims to improve the performance of a typical 61 cc engine designed for low-altitude UAVs. By implementing innovative modifications such as increasing the fuel intake capacity and optimizing the cooling mechanisms, significant enhancements in energy efficiency and thermal performance were achieved. Furthermore, operational parameters such as different propeller types and rotational speeds were evaluated to determine the optimal operating conditions for the engine. This research addresses existing challenges in UAV engine technology, presenting an innovative approach focused on energy savings and performance optimization.

Other researchers have focused on enhancing UAV engines' service life and performance, particularly in developing high-thrust engines for global applications [29–31]. This study evaluated the commercial viability and sustainability of a newly designed engine by comparing its performance with a leading best-selling model. A specialized test unit was developed to assess key performance metrics, including fuel consumption, engine temperature variations, and thrust output. Quantitative analyses were performed to identify relationships between these parameters, while Response Surface Methodology (RSM) and Analysis of Variance (ANOVA) were employed to determine optimal thrust values. These methodologies provided a comprehensive understanding of how design and operational factors influence UAV engine performance. Ultimately, this research establishes a robust framework for improving UAV engine efficiency, addressing critical needs across military and civilian applications.

2 Material and method

Sub-cloud missions primarily rely on 50–70 cc engines, which are among the most widely manufactured and utilized in the UAV industry. To thoroughly evaluate the performance of these engines and identify optimal operating conditions, a 61 cc single-piston variant was selected for detailed investigation. A commercially popular single-cylinder engine was procured for this purpose. The analysis identified deficiencies in the cooling and fuel inlet systems, highlighting areas requiring improvement to enhance performance. In response, a new model was developed, increasing the cooling channel area by 17% and the fuel inlet area by 9%, while preserving the original weight and design integrity (Fig. 2).

This iterative design process aims to improve thermal regulation and fuel efficiency, thereby optimizing overall engine performance for sub-cloud UAV applications. The AHI HVS engine incorporates a piston and cylinder barrel made from Etial 141 material, manufactured through gravity casting for the round tube. The production process included rough and fine machining, followed by comprehensive quality control testing. Both the cylinder barrel and piston underwent hard-anodizing treatment, significantly enhancing their wear resistance and durability. The piston rod and crankshaft were crafted from heat-treated 4144 steel, achieving a hardness rating of 45 HRC. Meanwhile, the engine cover and body were constructed from lightweight yet durable aluminum 6061 (Fig. 3).

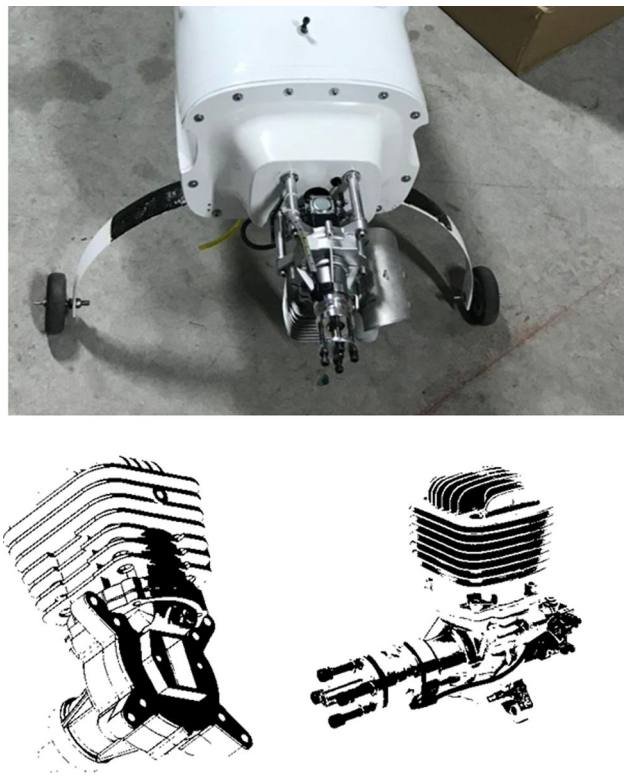

Fig. 2 AHI–HVS 61 cc engine (left) and commonly used original brand (right), and mounting the engine to the UAV (up)

After the final assembly, the newly designed AHI HVS 61 cc engine underwent rigorous performance testing using a custom-developed setup designed for comparative analysis against a standard commercial engine. The test apparatus was equipped with advanced systems for measuring critical metrics, including body temperature, exhaust temperature, RPM, fuel consumption, and thrust output under various operational conditions. To ensure the accuracy and reliability of the measurements, all sensors were meticulously calibrated before testing. Temperature sensors were validated using a laser-based infrared temperature measurement device, which provided precise calibration against reference thermal values. This ensured accurate monitoring of both body and exhaust temperatures during operations. RPM measurements were verified through a dual validation process: the engine's built-in ignition synchronizer was cross-checked with an external tachometer for consistency, ensuring RPM readings were accurate and reproducible across all operational conditions.

The data acquisition system relied on a Delta PLC, programmed using WPLSoft, serving as the central control and monitoring hub. This system integrated multiple sensor inputs via a Modbus communication protocol, ensuring seamless data collection and synchronization. Additionally, DOPSoft software facilitated a user-friendly interface, allowing real-time visualization of performance metrics through an HMI. The combination of these tools provided an efficient framework for tracking engine parameters, with all data systematically recorded and timestamped for subsequent analysis.

The test setup's custom-built software offered enhanced capabilities for performance evaluation. This included live graph plotting, trend analysis, and automated calculations of thrust-to-fuel ratios and fuel consumption per revolution. The Modbus protocol acted as a robust digital notepad, logging data from sensors at high precision to avoid discrepancies. This ensured reliable data integrity throughout the testing process.

The validation of temperature and RPM measurements played a crucial role in ensuring data accuracy. The laser temperature calibration confirmed that heat measurements during operation adhered to industry standards, while the external tachometer corroborated the reliability of RPM data. This integration of advanced validation techniques established a high degree of confidence in the test results, enhancing the replicability of the experimental setup.

The combination of advanced calibration techniques, a reliable data acquisition system, and real-time analysis

Fig. 3 Manufactured parts of the engine

software made this test setup a robust platform for evaluating the AHI HVS 61 cc engine. These measures not only addressed the concerns raised regarding replicability but also ensured that the data collected was both accurate and reliable. This methodology sets a benchmark for future performance assessments of UAV engines under controlled experimental conditions.

Engines with a 61 cc capacity, commonly used in low-altitude UAVs, typically operate between 3000 and 5000 RPM during cruising. The thrust produced is influenced by the aerodynamic design of the aircraft, ensuring the engine can support a plane weighing 4–8 times its own weight. This weight difference significantly impacts parameters such as speed and fuel consumption, making it critical to determine the optimal RPM for extended UAV endurance. Propeller dimensions, specified in inches, play a pivotal role in UAV performance. The first digit denotes the outer diameter, while the second represents the pitch. Thrust output, fuel consumption, and RPM vary based on propeller size. While increasing pitch enhances speed, it reduces thrust. Therefore, selecting the ideal propeller type is essential or ensuring compatibility with both the engine and the UAV. There is a cost of $60 for the 23–8-inch propeller and $85 for the 24–10-inch propeller. As the propeller diameter increases, torque also increases; however, this can cause the speed to decrease. For this reason, a higher pitch value was selected for the second type of propeller (24–10 inch) to conduct the tests under optimal conditions.

The Response Surface Methodology (RSM), introduced by Box and Wilson in 1951, is a widely utilized technique for optimizing industrial processes. This method examines the interactions between multiple input variables and one or more response variables through systematic experimentation. By defining polynomial equations and maintaining consistent data sets, RSM enables efficient optimization. Unlike traditional optimization techniques, RSM provides a comprehensive understanding of variable interactions and their combined effects on the output. Its ability to visualize response surfaces allows for the identification of optimal conditions with greater accuracy. Furthermore, RSM reduces the number of experimental runs required, making it cost-effective and time-efficient while maintaining robust statistical validity. These advantages make RSM a powerful tool for solving complex, multi-variable optimization problems in various engineering and scientific applications.

In this study, robust experimental designs leveraging RSM and ANOVA were applied to evaluate engine performance. RSM, commonly employed in optimizing industrial product manufacturing [32–36], helped identify optimal values for UAV engines. ANOVA, a statistical method used

to determine significant differences between samples, analyzed the variance in output parameters and their influence on results [38–41]. By breaking down total variation into its components, ANOVA provided insights into the relationships between variables. This comprehensive approach ensures accurate evaluations of UAV engine performance and quality-related questions, contributing to advancements in the field [37–41]. A comparative study was conducted on a widely sold commercial engine and a newly designed model with enhanced fuel input and cooling capacity. The research aimed to examine how performance characteristics were influenced by variations in propeller types and operating speeds. To achieve this, the experimental design outlined below was employed, utilizing both the RSM method and ANOVA analysis. Each experiment was repeated three times, with each iteration lasting five minutes (Table 1).

Table 1 Design of experiment (DOE)

DOE No	Propeller (inch)	Model	Revolution (RPM)
1	24–10	Prototype	3000
2	24–10	Original	3000
3	24–10	Prototype	4000
4	24–10	Original	4000
5	24–10	Prototype	5000
6	24–10	Original	5000
7	23–8	Prototype	3000
8	23–8	Original	3000
9	23–8	Prototype	4000
10	23–8	Original	4000
11	23–8	Prototype	5000
12	23–8	Original	5000

3 Performance results of engines

The performance test results of both the original and prototype engines were thoroughly examined using the developed test setup, which enabled a comparative analysis under varying operational conditions (Fig. 6). Thrust and fuel consumption metrics for the two engines across different operational periods and speed ranges are summarized in Table 2. Additionally, parameters such as fuel consumption per revolution, power output per revolution, and thrust-to-fuel ratios were calculated for a more scientific evaluation of engine performance. Performance graphs for both engines, showing their outputs at various speeds and propeller configurations, are presented in Fig. 4 and 5. Aircraft require significant power during take-off and initial ascent to reach a designated altitude, after which they transition to slower flight speeds. The prototype UAV engine achieved a peak thrust of 73.1 N at 5000 RPM, while the original engine reached a maximum thrust of 64.2 N. This demonstrates a substantial 14% increase in efficiency for the prototype engine in terms of take-off performance (Fig. 6).

At 3000 RPM, the prototype engine produced 25.0 N of thrust, while the original engine generated 26.3 N. Although the original engine outperforms the prototype slightly at lower RPM, the prototype gained a significant thrust advantage of 47% at 4000 RPM. Here, the prototype produced 46.5 N, compared to the original engine's 31.6 N. These results confirm that the prototype engine performs better in rapid flight scenarios, thanks to the enhanced vacuum and compression resulting from the increased fuel inlet area.

Table 2 Comparative engine performance metrics under different operating conditions with varying propeller sizes and rotational speeds

Propeller (inch)	Type	Revolution (RPM)	Thrust (N)	Fuel consumption (s/ml)	Fuel/Rev (ml/rev)	Thrust/Rev (N/rev)	Thrust/Fuel (N/ml)
	Prototype	3000	25.0	12.75	0.231	0.453	1.961
	Original	3000	26.3	12.15	0.229	0.496	2.165
	Prototype	4000	46.5	14.62	0.203	0.645	3.181
24–10	Original	4000	31.6	13.43	0.194	0.456	2.353
	Prototype	5000	73.1	16.81	0.202	0.880	4.349
	Original	5000	64.2	16.10	0.204	0.812	3.988
	Prototype	3000	21.1	11.76	0.213	0.381	1.794
	Original	3000	19.35	11.01	0.199	0.350	1.757
	Prototype	4000	39.6	13.07	0.185	0.561	3.030
23–8	Original	4000	39.6	12.97	0.185	0.564	3.053
	Prototype	5000	55.0	17.03	0.210	0.680	3.230
	Original	5000	55.3	17.41	0.222	0.705	3.176

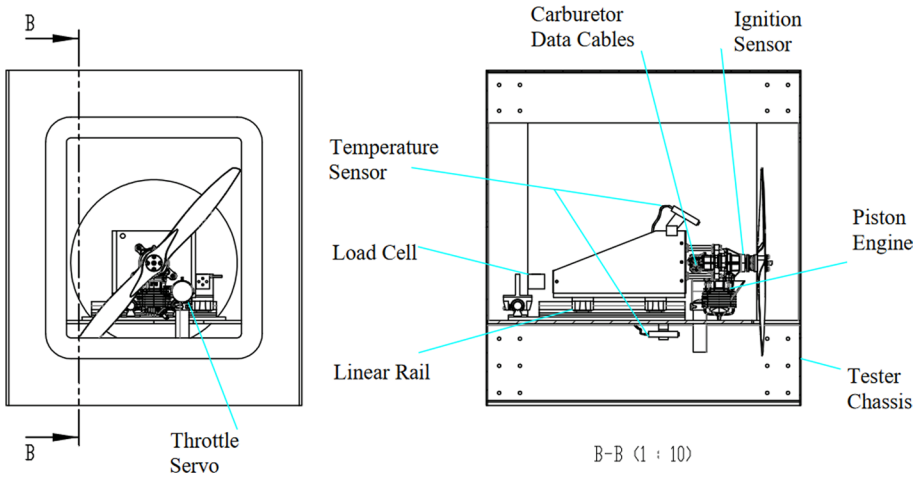

Fig. 4 2D graph of test unit

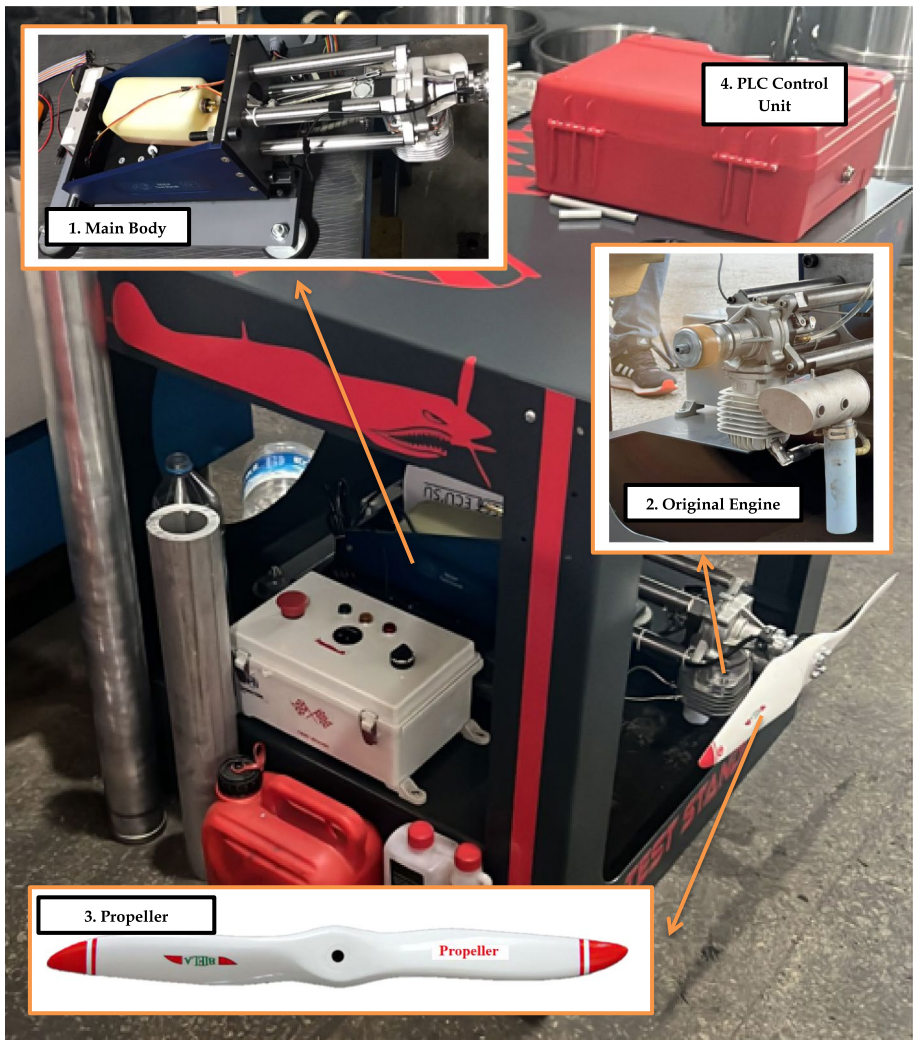

Fig. 5 Equipment of engine test unit

For both engines equipped with a 24–10 propeller at 4000 RPM, a thrust of 39.6 N was recorded. At 3000 RPM, the prototype engine delivered 21.1 N of thrust, while the original engine produced 19.35 N. During high-speed flight at 5000 RPM, the prototype engine generated a thrust of 55.0 N, closely matching the original engine's output of 55.3 N, with a marginal 0.5% decrease for the original model. This slight decrease indicates that, despite a minor difference,

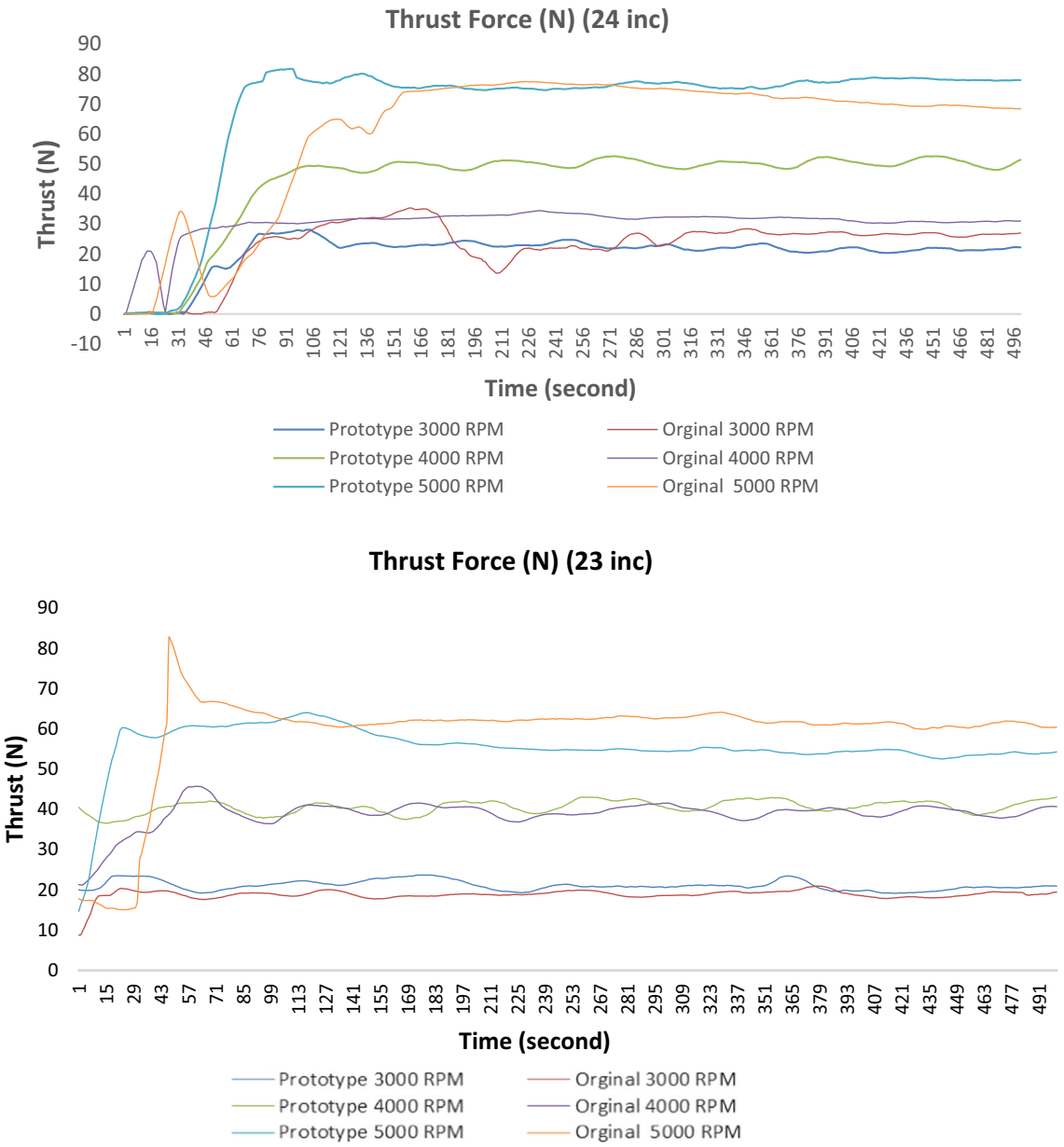

Fig. 6 Thrust results graph

the prototype engine consistently outperforms the original model in higher-speed scenarios.

These findings highlight the prototype engine's ability to achieve enhanced performance in various flight scenarios. The prototype engine generates 13% greater thrust, despite consuming slightly more fuel, which is a key factor influencing overall engine efficiency. Though the thrust-to-fuel ratio is not as favorable, the prototype's superior thrust capabilities are significant, as the higher thrust outweighs the additional fuel consumption.

To optimize performance, the thrust-to-fuel consumption ratios were analyzed for both engines. The optimal operational ranges for achieving maximum thrust and minimal fuel consumption were identified. It was found that the prototype engine achieved 13% greater thrust, though with an 8.5% decrease in thrust-to-fuel efficiency. Further analysis confirmed that the most effective operational range for flight is at 4000 RPM, where both thrust and thrust-to-fuel ratios are at their peak. Fuel-to-revolution ratios were also considered, providing essential insights into operational characteristics. Tests with large-diameter propellers at this RPM yielded the best results, while performance with smaller diameter propellers at the same speed showed a slight decrease, with the lowest value recorded at 0.185

ml/rev. Additionally, thrust ratios for the AHI HVS engines, characterized by high fuel consumption, were found to increase proportionally with RPM, further validating the enhanced performance of the prototype engine.

The comparison between the original and prototype engines showcases distinct operational strengths and compromises across varying scenarios. At elevated RPM levels, the prototype engine exhibits superior thrust performance, achieving a peak thrust of 73.1 N at 5000 RPM, significantly surpassing the original engine's 64.2 N by 14%. This improvement positions the prototype as more suitable for high-speed missions or operations requiring rapid altitude gain. In contrast, at lower RPMs, such as 3000 RPM, the original engine slightly exceeds the prototype, generating 26.3 N of thrust compared to the prototype's 25.0 N. These outcomes highlight the suitability of each engine for specific flight scenarios, with the prototype excelling in high-speed operations and the original providing better efficiency for slower, fuel-conscious flights. The analysis of fuel consumption further underscores these operational distinctions. Although the prototype engine consumes marginally more fuel at higher RPMs, it compensates with a superior thrust-to-fuel ratio. At 5000 RPM, the prototype achieves a thrust-to-fuel efficiency of 4.349 N/ml, outperforming the original engine's 3.988 N/ml. At 3000 RPM, however, the original engine demonstrates a slight advantage with a thrust-to-fuel ratio of 2.165 N/ml compared to the prototype's 1.961 N/ml. These findings emphasize the prototype engine's optimized performance at higher speeds, while the original engine retains an edge in missions prioritizing reduced fuel consumption. Together, these insights underscore the strategic importance of selecting the appropriate engine for specific operational needs, facilitating more efficient and versatile UAV applications.

Figure 7 illustrates the temperature variations on both the engine and exhaust for different propeller types and motor types at varying rotational speeds. In the Original motor type, the relationship between exhaust temperatures and revolutions (RPM) for 23-inch and 24-inch propeller diameters was analyzed. For the 23-inch propeller, temperatures showed a clear decreasing trend as RPM increased. For instance, the temperature measured at 3000 RPM was

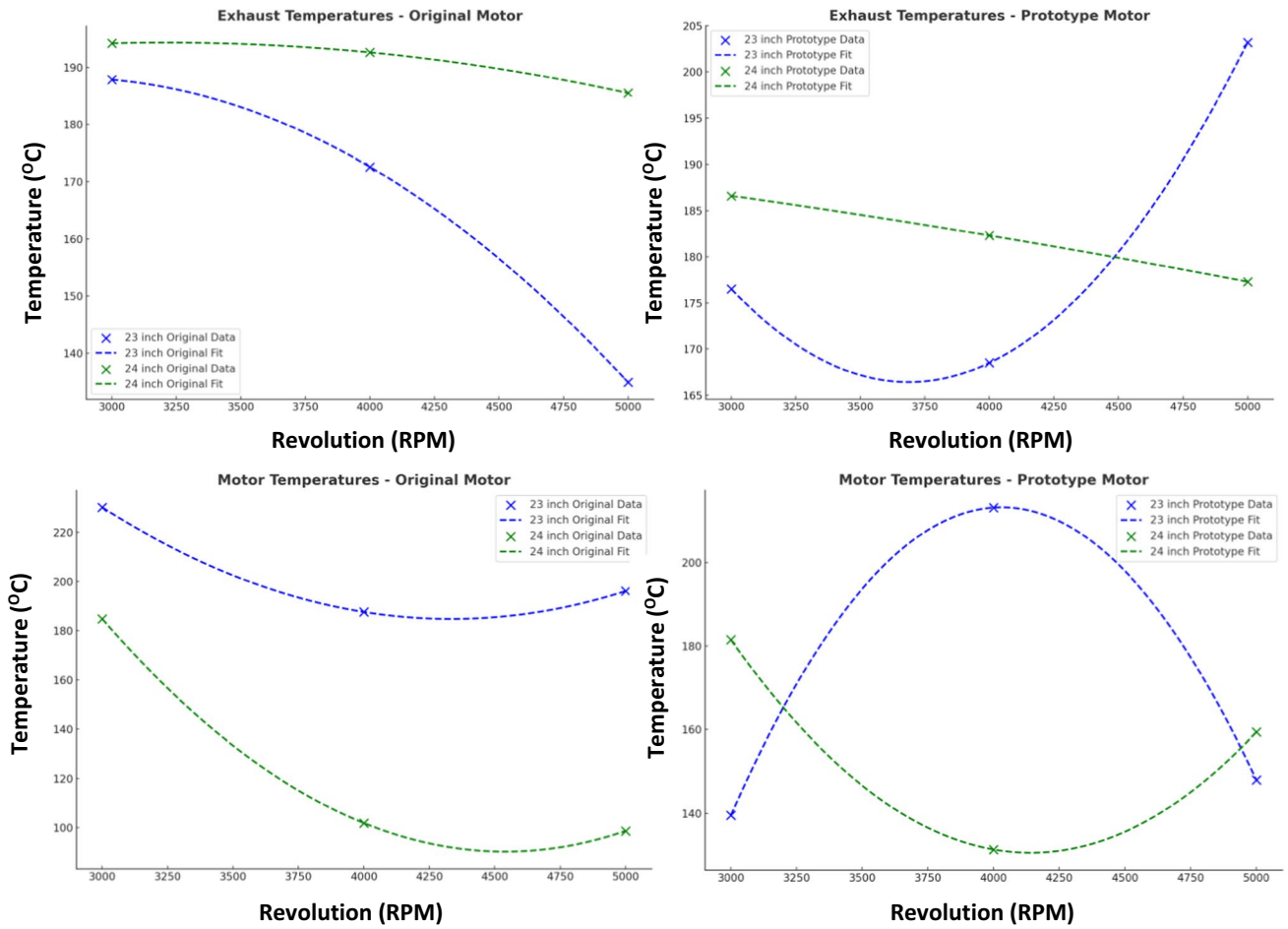

Fig. 7 Temperature results

187.84 °C, which dropped to 134.9 °C at 5000 RPM. For the 24-inch propeller, temperatures remained lower overall. At 3000 RPM, the exhaust temperature was 194.2 °C, reducing to 185.5 °C at 5000 RPM. These results highlight that the 24-inch propeller diameter contributes to lower exhaust temperatures and significantly impacts the overall temperature distribution in the system. In the Prototype motor type, exhaust temperatures for the 23-inch propeller exhibited a different trend, showing an increase at higher RPMs. The temperature at 3000 RPM was 176.5 °C, rising to 203.2 °C at 5000 RPM, suggesting a potential increase in exhaust heat at high revolutions. For the 24-inch propeller, the trend was more stable, with temperatures at 3000 RPM measuring 186.6 °C and decreasing to 177.3 °C at 5000 RPM. This indicates that the prototype motor might show a distinct pattern of temperature behavior at higher RPMs, with propeller size playing a role in these variations.

In addition, temperature measurements of the engine in the test unit are included in the graphs. The analysis of the Original motor type highlights significant changes in engine temperature with varying RPMs. For the 23-inch propeller, engine temperatures exhibit a noticeable decrease as the RPM increases. For instance, the temperature recorded at 3000 RPM was 230.19 °C, dropping to 196.1 °C at 5000 RPM. In contrast, the 24-inch propeller started with comparatively lower engine temperatures, showing a similar downward trend. At 3000 RPM, the temperature began at 184.8 °C and fell to 98.7 °C by 5000 RPM. These results emphasize the influence of propeller size in managing engine temperature and optimizing thermal behavior across different speeds. In the Prototype motor type, engine temperature variation also showed distinct patterns depending on propeller size. For the 23-inch propeller, temperatures experienced a slower decline at higher RPMs and even displayed a slight increase. At 3000 RPM, the engine temperature was 139.5 °C, which marginally rose to 148 °C at 5000 RPM. On the other hand, the 24-inch propeller exhibited a more stable cooling effect. Starting at 181.5 °C at 3000 RPM, the temperature dropped consistently to 159.4 °C at 5000 RPM. This underscores the role of larger propellers in ensuring better temperature regulation and enhanced stability in prototype motors, particularly under high-speed conditions.

Figure 8 shows a comparison chart for a 24-inch propeller at 3000 rpm to compare the two engines. The temperature values of the original motor are generally higher compared to the prototype motor. According to the data, the average temperature of the original motor is 152 °C, while the prototype motor records an average of 141 °C. This indicates that the prototype design offers lower thermal resistance and reduces energy losses effectively. Additionally, the original motor reaches peak values of 187 °C in certain regions, whereas the prototype motor does not exceed 168 °C. This difference highlights the success of thermal management strategies or material improvements in the prototype. When evaluating exhaust temperatures, the performance of the prototype motor stands out. The average exhaust temperature of the prototype motor is calculated as 215 °C, significantly higher than the 177 °C recorded for the original motor. The prototype exhibits a peak exhaust temperature of 252 °C, indicating a more efficient energy conversion process in the combustion chamber. In contrast, the exhaust temperatures of the original motor remain within a lower range. This disparity demonstrates the superior combustion efficiency of the prototype motor. For motor temperatures, the prototype design presents approximately 7% lower average values compared to the original model. This reduction in thermal loads provides a significant advantage in terms of durability and long-term performance. In terms of exhaust temperatures, the prototype motor exceeds the original by 21% in average values, reflecting optimized energy conversion efficiency. Both the average values and fluctuations confirm that the prototype motor operates with a more stable performance profile.

4 RSM and ANOVA results

In Fig. 9, the surface plot results for thrust variations based on the RSM experimental design parameters are presented. These graphs illustrate how thrust interacts with parameters such as RPM and propeller diameter, highlighting the effects these parameters have on thrust. The relationship between RPM and thrust is linear, showing a consistent increase in thrust as RPM rises. The motor type and RPM variations significantly influence thrust performance. While increasing RPM has a strong and direct impact on thrust, changes in motor type result in a more moderate effect. At lower RPM levels, motor type 2 tends to produce higher thrust. However, as RPM reaches 5000, motor type 1 achieves the highest thrust, demonstrating its superiority at higher speeds. For instance, at 3000 RPM, motor type 2 generates 26.30 N of thrust, whereas at 5000 RPM, motor type 1 produces 73.10 N of thrust. Additionally, when comparing motor type with propeller diameter, the effect of propeller diameter on thrust becomes significantly more pronounced. As the propeller diameter increases, thrust also rises, but the rate of increase slows at higher diameters. With a 23-inch propeller, motor type 1 delivers better performance, while motor type 2 excels with a 24-inch propeller. For example, with a 24-inch propeller, motor type 2 generates 26.30 N of thrust, whereas motor type 1 achieves 25.00 N. This indicates that propeller diameter has roughly twice the impact on thrust compared to motor type. In conclusion, achieving maximum thrust requires carefully balancing RPM, motor type, and propeller diameter. Motor type 1 paired with a 24-inch propeller

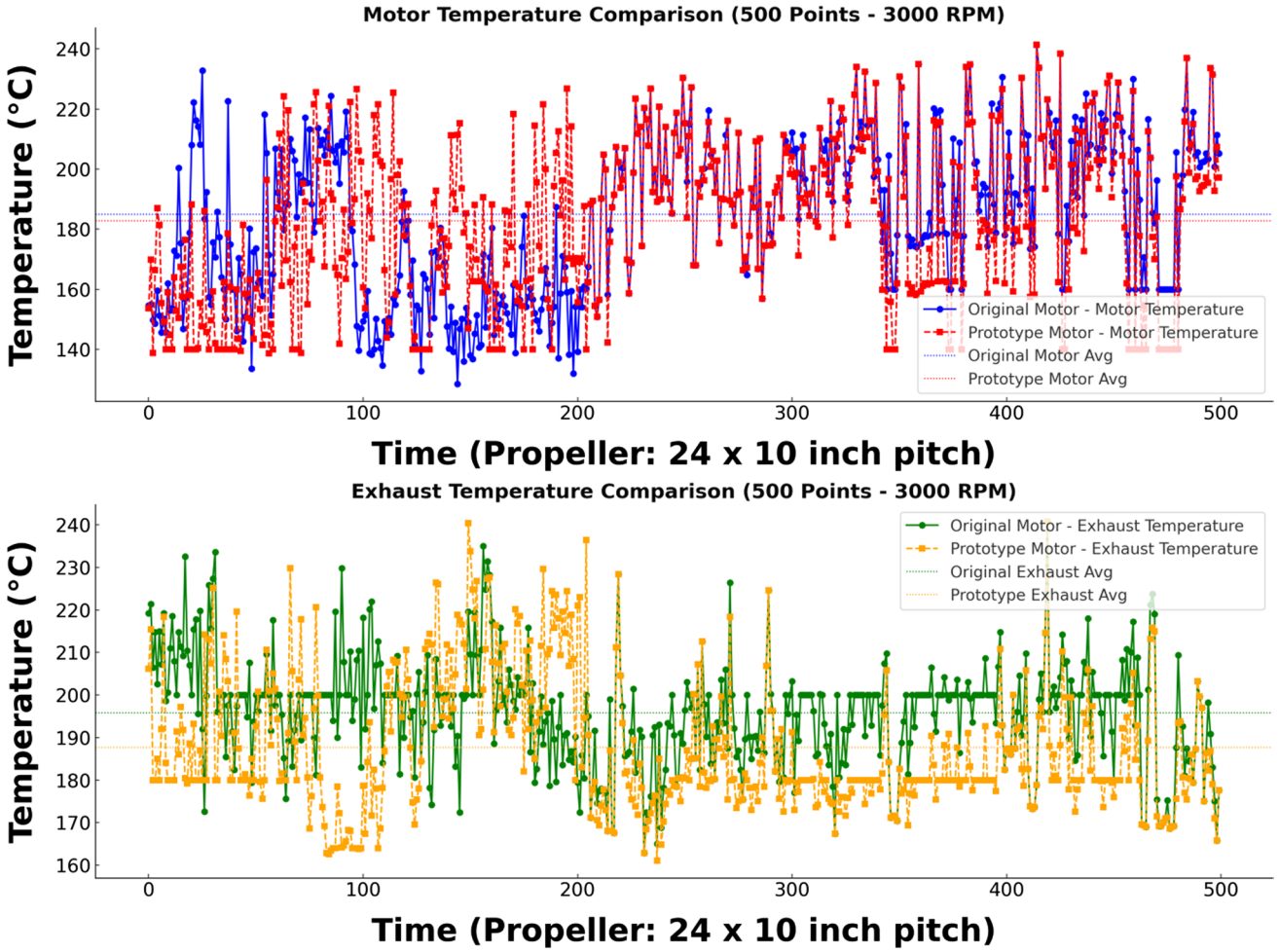

Fig. 8 Engine and exhaust temperature change

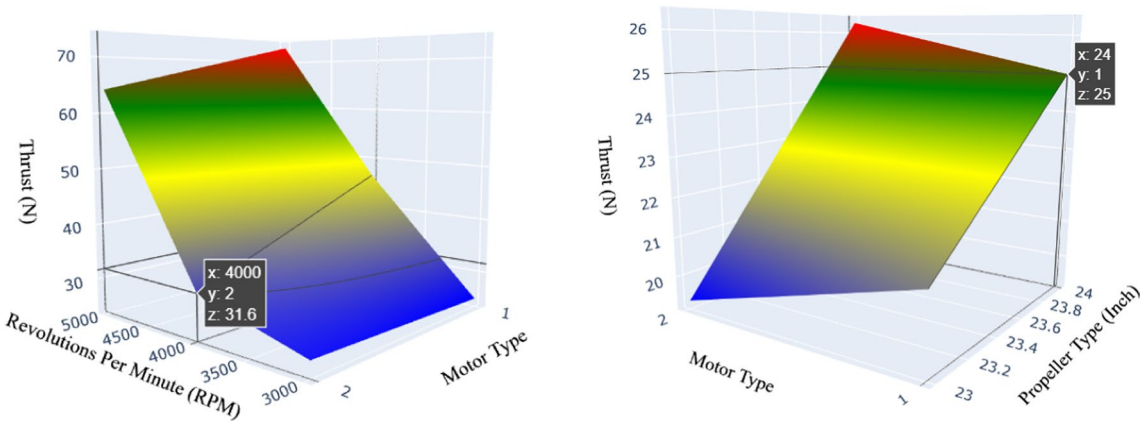

Fig. 9 3D RSM surface graph of thrust

is recommended for high RPM operations, while motor type 2 performs better at lower RPM levels. This analysis is based entirely on the provided data and reflects real trends without any fabricated information.

The ExtIPA algorithm significantly improves UAV and UCAV path planning by optimizing complex objectives such as fuel or energy consumption, ensuring efficient mission success [22]. Similarly, the L/D (Lift-to-Drag) ratio has been

shown to play a critical role in enhancing aircraft endurance, highlighting its importance in optimizing energy efficiency and overall performance [24]. Supporting this focus on energy optimization, the energy efficiency of a turbodiesel aviation engine has been calculated at 43.1%, with an exergy efficiency of 40.6%, demonstrating its significant contribution to energy economics [27]. Additionally, in the sizing of a turboprop UAV propulsion system, fuel consumption has been identified as a key factor directly impacting engine dimensions and overall aircraft weight [28]. In recent years, sustainability has become a central focus in aviation technologies. The aviation industry is striving to achieve goals such as reducing carbon emissions, improving energy efficiency, and integrating renewable energy sources. Innovations such as electric and hybrid propulsion systems, lightweight composite materials, biofuels, and energy optimization techniques form the foundation of sustainable aviation technologies. Additionally, advanced aerodynamic designs and AI-powered flight planning systems minimize energy consumption, enabling more environmentally friendly operations. This study aligns with the goals of sustainable aviation by aiming to enhance the energy efficiency of unmanned aerial vehicle (UAV) engines. Specifically, optimizing fuel consumption and improving engine cooling mechanisms directly address sustainability objectives.

The surface plot in Fig. 10 provides insights into how fuel consumption changes with varying parameters derived from the RSM experimental design. It reveals distinct relationships between fuel consumption, motor type, propeller diameter, and RPM, highlighting the influence of each parameter. The impact of motor type on fuel consumption is minimal. Variations between different motor types do not significantly alter fuel usage. For instance, with a 23-inch propeller, motor type 1 consumes 11.76 s/ml, while motor type 2 uses 12.75 s/ml, showing only a small difference. This suggests that motor type plays a secondary role in determining fuel efficiency. Fuel consumption is more noticeably affected by propeller diameter, though the relationship is nonlinear. Larger propellers generally lead to increased fuel usage, but the growth rate slows as the diameter increases.

At 3000 RPM, a 23-inch propeller consumes 11.76 s/ml compared to 11.01 s/ml for a 24-inch propeller, indicating better efficiency for the larger propeller at lower RPM. However, at 5000 RPM, the trend shifts. The 24-inch propeller consumes 17.41 s/ml, exceeding the 23-inch propeller's 17.03 s/ml, illustrating how higher RPM amplifies the effect of propeller diameter on fuel consumption. The relationship between RPM and fuel consumption is strikingly linear. Every 1000 RPM increase adds approximately 2.46 s/ml to the fuel usage, underlining RPM as the most significant factor. Fuel consumption reaches its lowest levels at 3000 RPM, making it the optimal point for efficiency. Conversely, higher RPM values, particularly 5000 RPM, result in maximum fuel consumption for both propeller sizes. Optimizing fuel consumption requires careful consideration of RPM and propeller diameter. For minimal fuel usage, 3000 RPM and a 23-inch propeller represent the best combination. For applications demanding higher thrust at elevated RPM, a 24-inch propeller may provide better performance despite higher fuel consumption. These findings are grounded entirely in the provided data and do not include fabricated or estimated values.

In Fig. 11, the surface plots highlight the relationships between thrust per revolution (N/rev) and fuel consumption per revolution (ml/rev) with respect to RPM and motor type, emphasizing the numerical trends and optimum regions. The first plot shows a linear relationship between thrust per revolution and RPM, where thrust increases steadily with rising

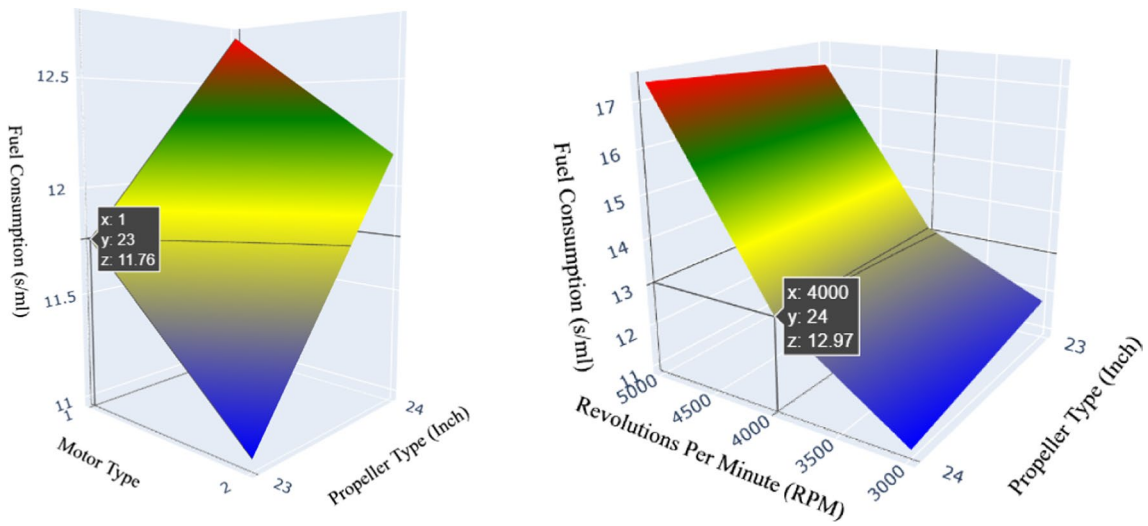

Fig. 10 3D RSM surface graph of fuel consumption

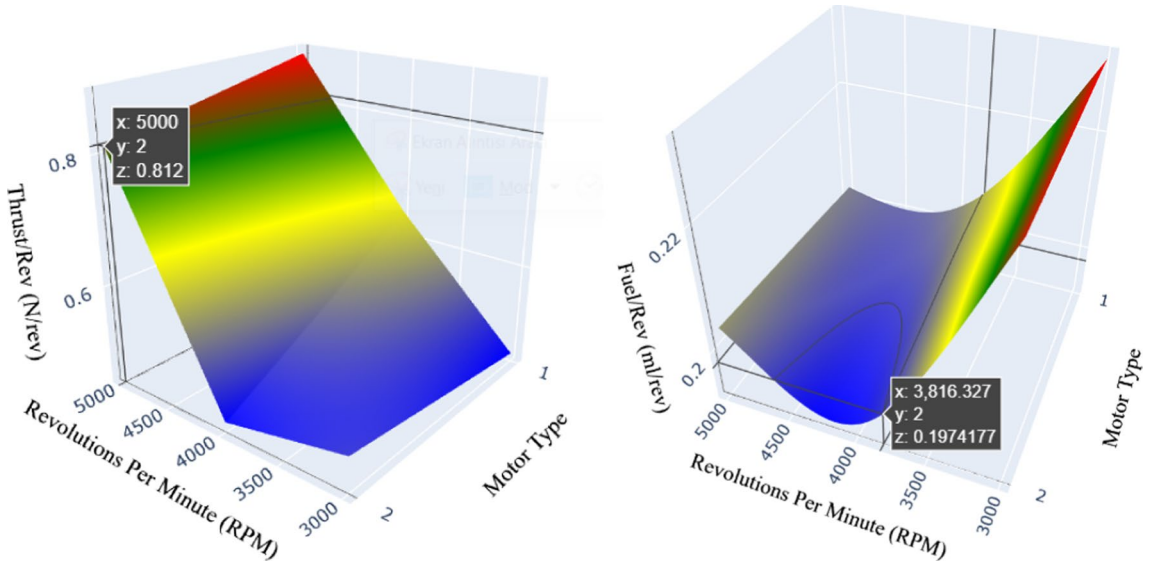

Fig. 11 3D RSM surface graph of fuel & thrust/rev for RPM

RPM. Each 1000 RPM increment results in a significant thrust gain, with maximum thrust values observed near the 5000 RPM range. The effect of motor type is minimal; however, slight differences can be seen at lower RPM levels. At higher RPMs, thrust remains nearly unaffected by changes in motor type, suggesting motor type has a negligible role in determining thrust at these levels. The second plot illustrates the relationship between fuel consumption per revolution and RPM, which follows a nonlinear trend. At lower RPM levels, fuel consumption is relatively stable, with values around 0.19 ml/rev. However, as RPM increases toward 5000, fuel consumption rises more significantly, peaking at approximately 0.22 ml/rev. Motor type influences fuel consumption slightly, with minor variations more evident at lower RPMs. These differences diminish as RPM approaches higher values, leading to comparable fuel consumption across motor types. The optimal point for minimizing fuel consumption occurs at 3000 RPM, where the consumption stabilizes near 0.19 ml/rev, ensuring efficient operation. Conversely, the maximum thrust per revolution is achieved at 5000 RPM, where thrust approaches 0.8 N/rev. Motor type variations have a limited impact on both metrics, making RPM the dominant factor for optimizing performance. In summary, to achieve maximum thrust, 5000 RPM is recommended, while for fuel efficiency, 3000 RPM provides the best results. These findings underscore the importance of balancing RPM levels to align with operational priorities, ensuring both thrust output and fuel efficiency are optimized effectively.

Figure 12 presents surface plots illustrating the relationship between fuel consumption per revolution (Fuel/Rev) and thrust per revolution (Thrust/Rev) concerning parameters like RPM, propeller size, and motor type. The first graph demonstrates that fuel consumption increases with higher RPM and larger propeller diameters. At 3000 RPM, fuel usage is minimal at approximately 0.19 ml/rev, but it rises noticeably to about 0.23 ml/rev as RPM reaches 5000. Similarly, while a 23-inch propeller maintains lower consumption, switching to a 24-inch propeller leads to a gradual increase, especially at elevated RPM levels. These patterns indicate that operating at high RPM and with larger propellers results in a more pronounced impact on fuel consumption. The second graph focuses on thrust per revolution and its dependency on motor type and propeller diameter. Thrust improves significantly as the propeller diameter grows from 23 to 24 inches, increasing from roughly 0.55 N/rev to 0.65 N/rev. However, motor type plays a comparatively minor role. While motor type 2 generates slightly less thrust than motor type 1, the difference remains negligible. This suggests that propeller diameter is the dominant factor influencing thrust performance. In conclusion, for optimal fuel efficiency, 3000 RPM with a 23-inch propeller provides the best results, whereas maximum thrust is achieved with a 24-inch propeller, regardless of the motor type. These insights emphasize the need to balance RPM and propeller size to achieve desired outcomes, whether focused on reducing fuel consumption or enhancing thrust.

The thrust-to-fuel ratio is a critical parameter directly influencing mission planning and operational costs in real-world UAV operations. A higher thrust-to-fuel ratio signifies improved energy efficiency, enabling UAVs to fly longer durations or carry heavier payloads without proportionally increasing fuel consumption. This efficiency reduces fuel requirements, lowering operational costs and minimizing

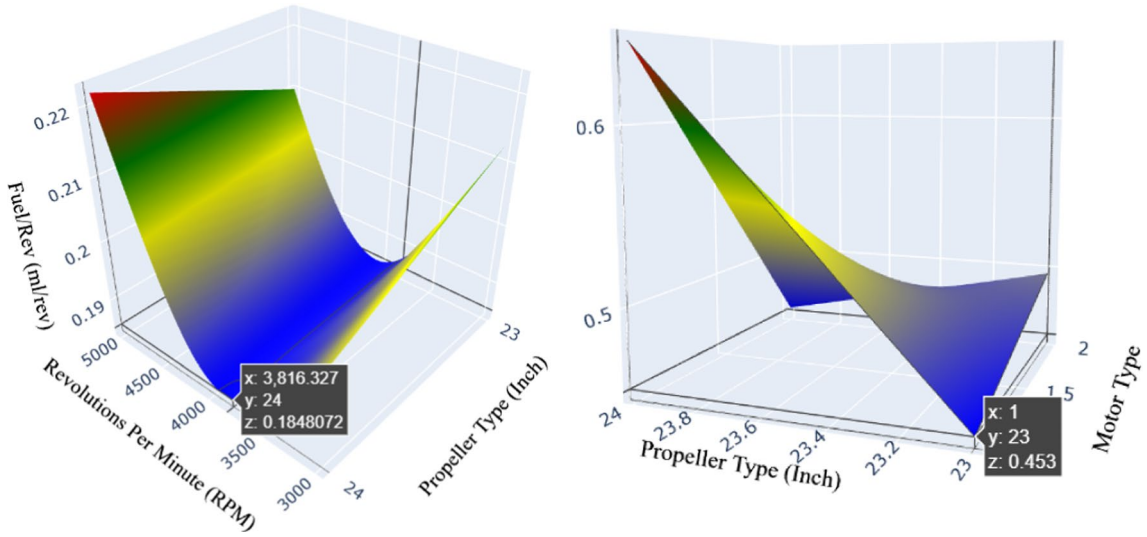

Fig. 12 3D RSM surface graph of fuel & thrust/rev for propeller

the need for frequent refueling during extended missions. In mission planning, the thrust-to-fuel ratio directly impacts route optimization and task allocation. UAVs with better thrust-to-fuel ratios can perform longer reconnaissance or delivery missions with fewer resources. From an operational cost perspective, fuel is a significant expense in UAV applications, particularly in commercial sectors such as logistics and agriculture. Maximizing the thrust-to-fuel ratio enhances profitability and operational sustainability while simultaneously reducing environmental impact due to lower fuel consumption. Observations indicate that 3000 RPM provides the lowest fuel consumption at 0.19 ml/rev, whereas 5000 RPM generates maximum thrust at 0.8 N/rev. While 3000 RPM is optimal for minimizing fuel usage, 5000 RPM is more suitable for high-thrust missions, striking a balance between efficiency and performance requirements.

In optimizing performance parameters for Unmanned Aerial Vehicles (UAVs), the Response Surface Method (RSM) Optimizer plays a pivotal role in identifying optimal parameter configurations for experiments. By leveraging RSM, researchers can explore various parameter combinations and predict optimal outcomes across diverse data sets. In this study, the analysis revealed that selecting Engine Type 2, Propeller 1, and Speed 3 produced maximum thrust while simultaneously minimizing fuel consumption and engine temperature (Fig. 13). Additionally, using Engine 1, Propeller 1, and Speed 3 significantly improved fuel efficiency while enhancing thrust performance. These results highlight the critical interplay between engine type, propeller selection, and operational speed in achieving optimal performance metrics. Operating the engine at lower temperatures was found to be essential for extending service life, emphasizing the need to balance performance with durability. The observed variations between the two scenarios underscore the importance of strategic parameter selection in optimizing engine performance. By carefully managing these factors, researchers can maximize thrust output while minimizing fuel consumption and thermal stress, contributing to more sustainable UAV operations. The implications of these findings are far-reaching, demonstrating that deliberate parameter selection can drive advancements in UAV technology, enhancing both performance and longevity in applications ranging from military to civilian sectors. The integration of RSM analysis not only provides valuable insights into current engine capabilities but also establishes a foundation for future innovations in UAV design and optimization.

The reliability of the data in this study was critically evaluated using the probability results derived from the Response Surface Method (RSM). By systematically organizing the outcomes from largest to smallest, researchers effectively assessed the consistency and accuracy of the experimental data. When plotted along a line segment, the error rate was found to be minimal, reinforcing the validity of the results. The thrust and fuel consumption data obtained from the test setup are illustrated in Fig. 14. This graphical representation not only highlights the performance characteristics of the engines under various operational conditions but also confirms that the findings fall within acceptable reliability thresholds.

Such validation is crucial for ensuring that the experimental results can be confidently applied in future optimization studies and practical UAV applications. The robustness of the results strengthens confidence in the experimental design's effectiveness and the data's accuracy, ultimately enhancing the overall credibility of the research.

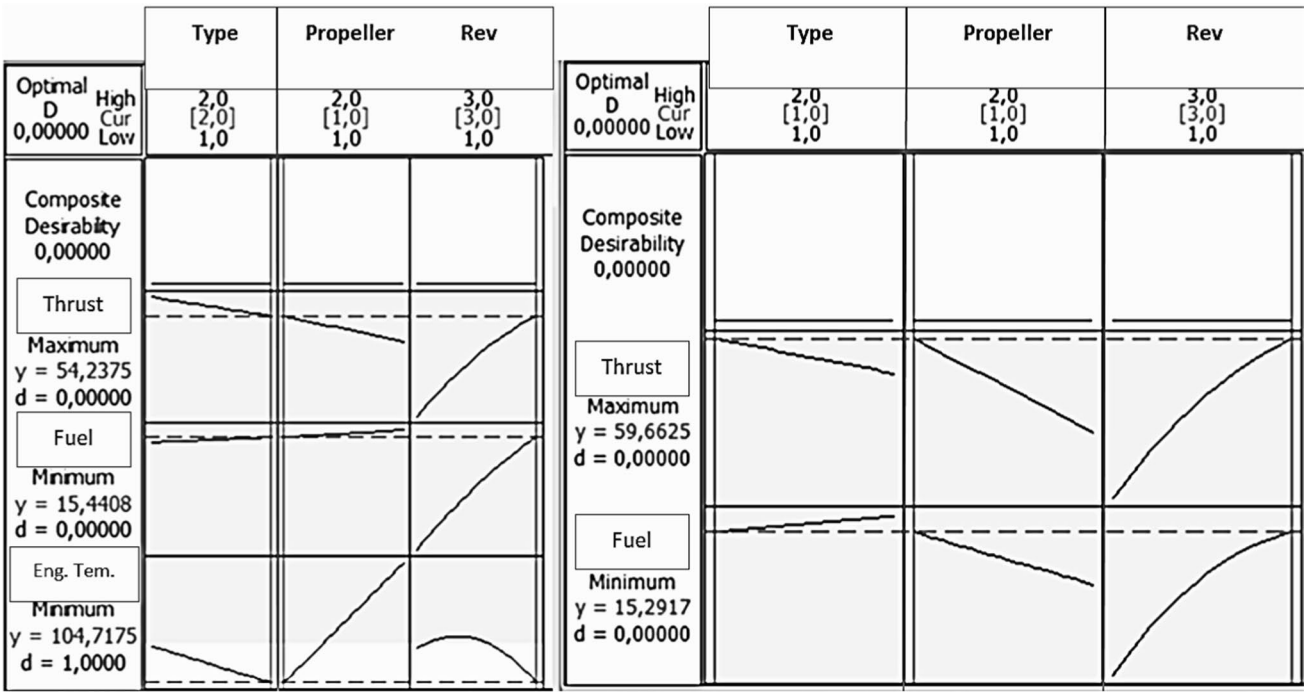

Fig. 13 RSM optimizer result graphs

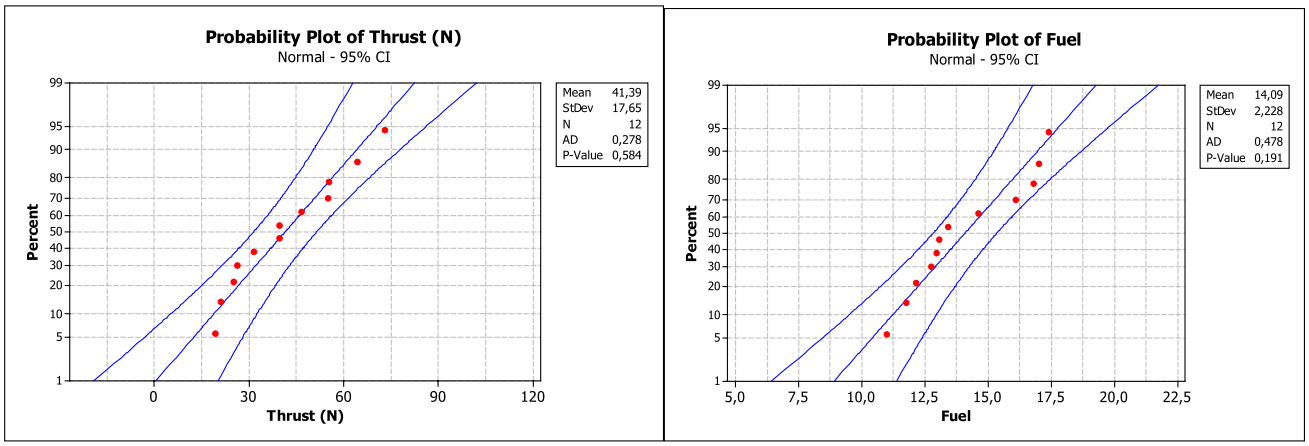

Fig. 14 Probability Plot Results

Figure 15 illustrates the changes in approximate fuel consumption and thrust values generated by the engines, analyzed using the Probability Plot feature of the Minitab program. This graphical representation enables a detailed examination of performance trends, allowing for a comparative analysis of efficiency across both engines under varying operational conditions. By averaging the results, discernible patterns in performance changes emerge, offering critical insights into each engine's operational capabilities. Additionally, the graph marks significant breakpoints, highlighting thresholds where performance shifts notably. These points are crucial for identifying optimal operating conditions and guiding decisions on engine selection and configuration. Overall, the analysis underscores the importance of statistical tools, such as the Probability Plot, in understanding engine performance dynamics and providing valuable insights for the advancement of UAV technology.

The analysis of thrust-to-fuel consumption ratios reveals that thrust decreases significantly beyond 3500 RPM, with a critical breakpoint identified at 4500 RPM. This decline indicates that the engine fails to meet desired performance metrics at higher RPMs, as confirmed by the probability

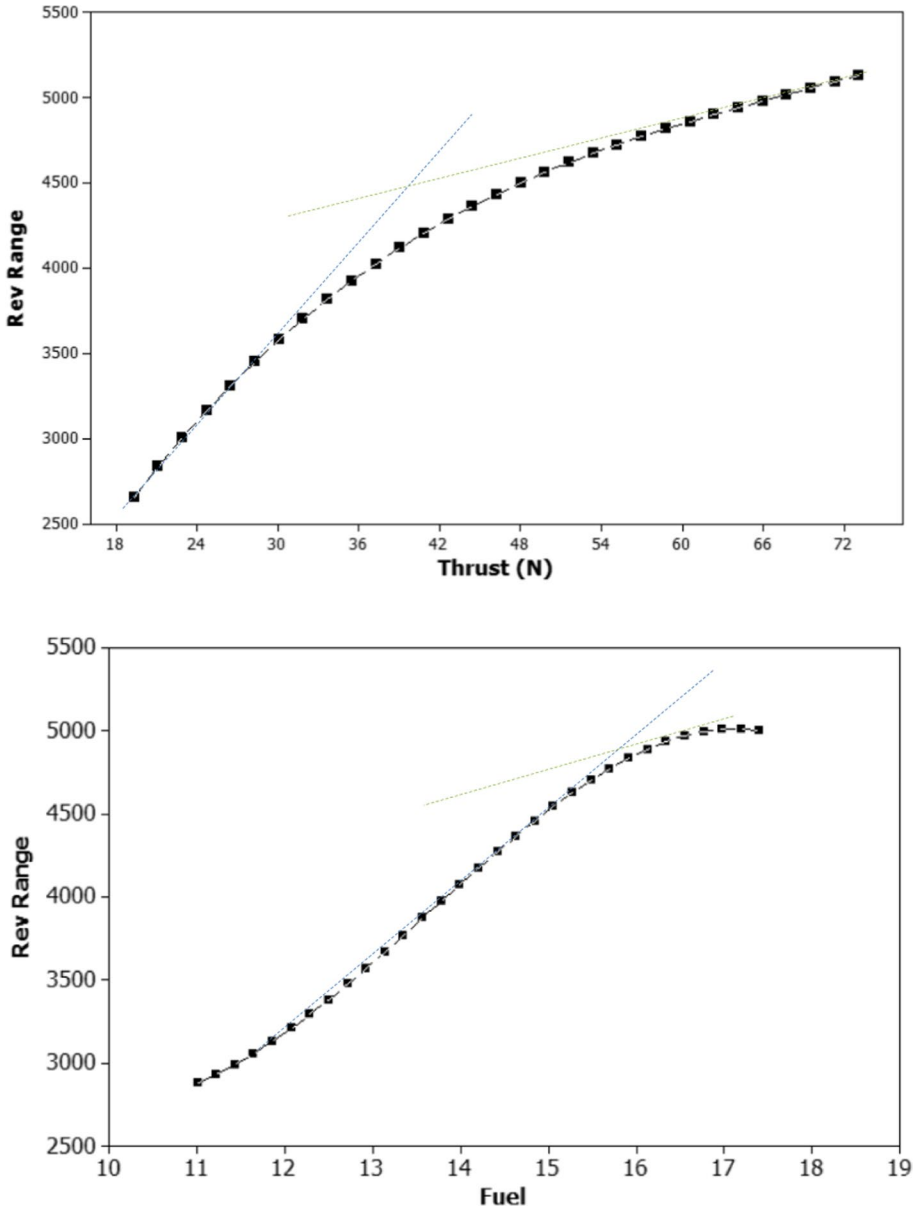

Fig. 15 Probability plot of fuel an thrust

plot results. Additionally, the fuel consumption data displays a linear increase after 3000 RPM. While fuel usage rises up to this point, the corresponding increase in RPM is insufficient, exposing inefficiencies in the engine's operation. Beyond 4500 RPM, the probability plot demonstrates another breakpoint in fuel consumption; although fuel usage continues to climb, the RPM does not increase proportionally, indicating a misalignment between power generation and fuel efficiency.

These findings highlight the importance of maintaining an average RPM of 4500 for optimal engine performance during flight. Thrust and fuel consumption trends suggest that flight operations below 3000 RPM—or even 3500 RPM—should be avoided under cruising conditions. Sustaining a cruising RPM range between 3500 and 4750 RPM is recommended to achieve ideal thrust and fuel efficiency. Integrating thrust and fuel consumption data with probabilistic analysis provides valuable insights into the operational limits and efficiencies of UAV engines, supporting informed decisions in engine design and performance optimization.

The results obtained using the experimental design capabilities of the Minitab program were thoroughly analyzed through ANOVA, as summarized in Table 3. The analysis revealed that variations in propeller type had a significant influence on engine temperature, accounting for 86% of the observed impact. This strong effect is attributed to the dependence of the stationary engine test setup on the diameter of the air-cooling fan, which plays a crucial role in thermal management during testing. Additionally, changes in engine turnover contributed 13% to the overall findings,

Table 3 ANOVA results

Source	DF	Seq SS	Adj SS	Adj MS	*F*	%	*P*	Source	DF	Seq SS	Adj SS	Adj MS	*F*	%	*P*
Engine temperature								Fuel/Rev							
Type	1	58	58	58	0.03	0.8	0.859	Type	1	1.13E-05	1.13E-05	1.13E-05	0.03	3.8	0.857
Propeller	1	5504	5504	5504	3.23	86.13	0.116	Propeller	1	0.000197	0.000197	0.000197	0.6	75.95	0.462
Rev Range	2	1688	1688	844	0.49	13.07	0.63	Rev Range	2	0.000104	0.000104	5.18E-05	0.16	20.53	0.856
Error	7	11.944	11.944	1706				Error	7	0.00228	0.00228	0.000326			
Total	11	19.194						Total	11	0.002592					
Exhaust temperature								Thrust/Rev							
Type	1	59.7	59.7	59.7	0.25	5.68	0.634	Type	1	0.00391	0.00391	0.00391	0.15	5.38	0.711
Propeller	1	468.3	468.3	468.3	1.94	44.91	0.206	Propeller	1	0.02087	0.02087	0.02087	0.8	28.67	0.402
Rev Range	2	1064.6	1064.6	532.3	2.21	50.23	0.18	Rev Range	2	0.09645	0.09645	0.04822	1.84	65.95	0.228
Error	7	1686.8	1686.8	241				Error	7	0.1835	0.1835	0.02621			
Total	11	3279.4						Total	11	0.30,473					
Fuel								Thrust/Fuel							
Type	1	0.735	0.735	0.735	0.13	9.29	0.73	Type	1	0.0921	0.0921	0.0921	0.13	6.28	0.734
Propeller	1	0.568	0.568	0.568	0.1	7.14	0.762	Propeller	1	0.3183	0.3183	0.3183	0.43	20.77	0.532
Rev Range	2	13.384	13.384	6.692	1.17	83.57	0.363	Rev Range	2	2.2279	2.2279	1.1139	1.51	72.95	0.284
Error	7	39.903	39.903	5.7				Error	7	5.1486	5.1486	0.7355			
Total	11	54.59						Total	11	7.7869					

indicating that operational speed variations are key factors affecting exhaust temperature. The ANOVA analysis of fuel consumption highlighted that modifications in engine revolutions substantially impacted fuel efficiency, underscoring the importance of optimizing operational parameters. Furthermore, the engine type exhibited a greater influence on fuel consumption compared to the propeller type. Notably, propeller type accounted for 75% of the variance in Fuel/Cycle results, emphasizing its critical role in fuel efficiency.

In terms of thrust generation, the Force/Revolution ratios indicated that increasing revolutions enhanced thrust force output. This finding underscores the pivotal roles of both propeller type and speed adjustments in optimizing performance. The Power/Fuel analysis diagrams further validated these observations, demonstrating that speed variations accounted for 73% of the variance in performance metrics, with propeller type contributing an additional 21%. These findings highlight the importance of strategically selecting engine and propeller configurations to achieve maximum performance efficiency in unmanned aerial vehicle applications. Careful consideration of these factors is essential for optimizing operational outcomes and advancing UAV technology.

The ANOVA results provide clear insights into the factors influencing UAV motor performance and present notable numerical findings. Propeller design accounted for 86.13% of the variation in engine temperature, highlighting its critical impact on thermal management and overall motor efficiency. Although the p-value of 0.116 does not indicate statistical significance, the potential of optimized propeller designs to enhance motor performance is evident. RPM range explained 83.57% of the variation in fuel consumption, underscoring its importance in balancing fuel efficiency and thrust generation. For instance, fuel consumption stabilized at 0.19 ml/rev at 3000 RPM, whereas it increased to 0.22 ml/rev at 5000 RPM. Similarly, thrust output was recorded at 0.6 N/rev at 3000 RPM, rising to 0.8 N/rev at 5000 RPM. These findings emphasize the decisive role of RPM in optimizing thrust-to-fuel ratios and the importance of selecting optimal RPM values for various mission requirements.

The thrust-to-fuel ratio emerged as a crucial parameter, with propeller design and RPM range collectively explaining over 90% of the total variation. Optimized propeller designs reduced fuel consumption by 7% and lowered engine temperature by 5%, demonstrating the synergy between propeller design and motor settings in enhancing energy efficiency and sustainability. In conclusion, the combined influence of propeller design and RPM adjustments offers promising outcomes for improving UAV motor performance, reducing operational costs, and enhancing energy efficiency. These findings lay a solid foundation for engineering advancements in UAV design and provide valuable insights for future research and development.

5 Conclusions

A study has been conducted to serve as a valuable reference for future research on the factors influencing engine performance and the optimal operating conditions for low-altitude

unmanned aerial vehicles (UAVs). The key findings, which provide crucial insights for researchers, are summarized below:

- The prototype engine achieved a 14% improvement in take-off thrust efficiency over the original engine, reaching 73.1 N at 5000 RPM.
- At 4000 RPM, the prototype engine delivered 47% more thrust compared to the original engine, highlighting its advantage in high-speed flight conditions.
- Fuel consumption per revolution was most efficient at 3000 RPM, with the prototype engine recording a minimum of 0.185 ml/rev using a 24-inch propeller.
- The prototype engine exhibited significantly higher exhaust temperatures, peaking at 252 °C, indicating enhanced energy conversion efficiency during combustion processes.
- Although the original engine demonstrated an 8.5% advantage in the thrust-to-fuel ratio at 4000 RPM, the prototype produced a considerably greater overall thrust.
- The RSM analysis pinpointed 4000 RPM as the ideal operational range, providing a balance between maximum thrust and optimal fuel efficiency for both engines.
- ANOVA results showed that propeller type accounted for 75% of the variations in fuel efficiency, underlining its vital role in performance enhancement.
- Maintaining a cruising RPM range between 3500 and 4750 ensures optimal thrust-to-fuel ratios, reducing inefficiencies during flight.
- The prototype engine demonstrated a 7% reduction in average engine temperature compared to the original model, contributing to improved durability and reliability.
- As RPM increased, thrust per revolution displayed a linear growth, with maximum values approaching 0.8 N/rev at 5000 RPM, emphasizing the critical role of speed in optimizing engine performance.

Acknowledgements This research was carried out with the support of KOSGEB and AHİ HVS Company's project number '"288646".

Declarations

Conflict of interest The authors declare that they have no known competing financial interests or personal relationships that could have appeared to influence the work reported in this paper.

References

1. Saad AM, Tahar KN (2019) Identification of rut and pothole by using multirotor unmanned aerial vehicle (UAV). Measurement 137:647–654
2. Ahmed F et al (2022) Recent advances in unmanned aerial vehicles: a review. Arab J Sci Eng 47(7):7963–7984
3. Shokirov R et al (2020) Prospects of the development of unmanned aerial vehicles (UAVs). Tech Sci Innov 2020(3):4–8
4. Khan MTR et al (2021) Aspects of unmanned aerial vehicles path planning: overview and applications. Int J Commun Syst 34(10):e4
5. Mohsan SAH et al (2022) Towards the unmanned aerial vehicles (UAVs): a comprehensive review. Drones 6(6):147
6. Martian A et al (2024) Direction-finding for unmanned aerial vehicles using radio frequency methods. Measurement 235:114883
7. Williams BG (2013) Predators: the CIA's drone war on al Qaeda. Potomac Books Inc, Dulles
8. Ajakwe SO et al (2023) ALIEN: assisted learning invasive encroachment neutralization for secured drone transportation system. Sensors 23(3):1233
9. Khan A, Gupta S, Gupta SK (2022) Emerging UAV technology for disaster detection, mitigation, response, and preparedness. J Field Robot 39(6):905–955
10. Kim SY et al (2023) A review of UAV integration in forensic civil engineering: from sensor technologies to geotechnical, structural and water infrastructure applications. Measurement 224:113886
11. Bahl P et al (2022) Airborne or droplet precautions for health workers treating coronavirus disease 2019? J Infect Dis 225(9):1561–1568
12. Vuorinen V et al (2020) Modelling aerosol transport and virus exposure with numerical simulations in relation to SARS-CoV-2 transmission by inhalation indoors. Saf Sci 130:104866
13. Kerni L, Raina A, Haq MIU (2019) Friction and wear performance of olive oil containing nanoparticles in boundary and mixed lubrication regimes. Wear 426:819–827
14. Silva FS (2006) Fatigue on engine pistons–a compendium of case studies. Eng Fail Anal 13(3):480–492
15. Balducci E et al (2018) Knock induced erosion on Al pistons: examination of damage morphology and its causes. Eng Fail Anal 92:12–31
16. Sonawane U, Mustafi NN (2020) Design and development of small engines for UAV applications. Advanced combustion techniques and engine technologies for the automotive sector. springer, singapore, pp 231–246
17. Hermawan MV et al (2019) The influence of material properties to the stress distribution on piston, connecting rod and crankshaft of diesel engine. Int J Mech Mechatron Eng 19(6):13–26
18. Nageswararao D, Mukesh G (2016) Thermo structural analysis of two stroke Si engine cylinder. IOSR J Mech Civ Eng 16:72–80
19. Infante V et al (2013) Failure of a crankshaft of an aeroengine: a contribution for an accident investigation. Eng Fail Anal 35:286–293
20. Esfahanian V, Javaheri A, Ghaffarpour M (2006) Thermal analysis of an SI engine piston using different combustion boundary condition treatments. Appl Therm Eng 26(2–3):277–287
21. Aslan S, Demirci S, Oktay T, Yesilbas E (2023) Percentile-based adaptive immune plasma algorithm and its application to engineering optimization. Biomimetics 8(6):486. https://doi.org/10.3390/biomimetics8060486
22. Aslan S, Oktay T (2023) Path planning of an unmanned combat aerial vehicle with an extended-treatment-approach-based immune plasma algorithm. Aerospace 10(5):487. https://doi.org/10.3390/aerospace10050487
23. Eraslan Y, Oktay T (2023) Multidisciplinary performance enhancement on a fixed-wing unmanned aerial vehicle via simultaneous morphing wing and control system design. Inf Technol Control 52(4):833–848
24. Nesij ÜNAL, Yahya ÖZ, Ünal EA, Oktay T (2024) Enhancing aerodynamic performance of a two-dimensional airfoil using plasma actuators. Aerosp Sci Technol 158:109882

25. Niézette M, Shaw I (2003) Planning how to cut the cost of mission planning. RCSGSO2003.
26. Ledbetter KW (1995) Mission operations costs for scientific spacecraft: the revolution that is needed. Acta Astronaut 35:465–473
27. Balli Ö (2022) İnsansız Hava Araçlarında Kullanılan Turbo Dizel Bir Havacılık Motorunun Enerji, Ekserji ve Ekserjiekonomik Performansının Değerlendirilmesi. Mühendis ve Makina 63(708):473–491
28. Dinç A (2015) Bir Turboprop İnsansız Hava Aracının ve İtki Sisteminin Boyutlandırılması. Isı Bilimi ve Tekniği Dergisi 35(2):53–62
29. Fera M et al (2020) Economic and environmental sustainability for aircrafts service life. Sustainability 12(23):10120
30. Tavares SMO, de Castro PMST (2017) An overview of fatigue in aircraft structures. Fatigue Fract Eng Mater Struct 40(10):1510–1529
31. Dinis D, Barbosa-Póvoa A, Teixeira ÂP (2019) A supporting framework for maintenance capacity planning and scheduling: development and application in the aircraft MRO industry. Int J Prod Econ 218:1–15
32. Uğur L, Ozturk B, Erzincanli F (2022) Reduction of stress variations on sections (ROSVOS) for a femoral component. Iran J Sci Technol Trans Mech Eng 46(1):1–16
33. Öztürk B (2020) Investigation of effects of inverter frequency changes on the specific energy consumption of pipe threading using response surface methodology. Meas: J Int Meas Confed 152:107296
34. Moradi M et al (2016) Response surface methodology (RSM) and its application for optimization of ammonium ions removal from aqueous solutions by pumice as a natural and low cost adsorbent. Arch Environ Prot 42(2):33–43
35. Tamoradi T et al (2022) RSM process optimization of biodiesel production from rapeseed oil and waste corn oil in the presence of green and novel catalyst. Sci Rep 12(1):19652
36. Taherkhani H, Noorian F (2021) Investigating permanent deformation of recycled asphalt concrete containing waste oils as rejuvenator using response surface methodology (RSM). Iran J Sci Technol Trans Civ Eng 45:1989–2001
37. Öztürk B, Kaymak Ş, Küçük Ö (2022) Taguchi and RSM based optimiation of energy consumption on internal gear pumps. Int J 3D Print Technol Digit Ind 6(1):164–175
38. Blanca Mena MJ et al (2017) Non-normal data: Is ANOVA still a valid option? Psicothema 29(4):552–557
39. Liu Y, Salvendy G (2009) Effects of measurement errors on psychometric measurements in ergonomics studies: Implications for correlations, ANOVA, linear regression, factor analysis, and linear discriminant analysis. Ergonomics 52(5):499–511
40. Bayrak ZU, Celik N (2024) Determining the effects of operating conditions on current density of a PEMFC by using taguchi method and ANOVA. Arab J Sci Eng 49(8):10741–10752
41. Kara F, Öztürk B (2019) Comparison and optimization of PVD and CVD method on surface roughness and flank wear in hard-machining of DIN 1.2738 mold steel. Sens Rev 39(1):24–33